Assessment of freeze-thaw resistance of cement based concrete with ground glass – pozzolan through X-ray microtomography

Krstic, Marija; Davalos, Julio F.; Rossi, E.; Chaves Figueiredo, S.; Copuroglu, Oguzhan

Publication date
2021

Document Version
Final published version

Published in
4th International Rilem Conference on Microstructure Related Durability of Cementitious Composites

Citation (APA)
Krstic, M., Davalos, J. F., Rossi, E., Chaves Figueiredo, S., & Copuroglu, O. (2021). Assessment of freeze-thaw resistance of cement based concrete with ground glass – pozzolan through X-ray microtomography. In G. Ye, H. Dong, J. Liu, E. Schlangen, & C. Miao (Eds.), *4th International Rilem Conference on Microstructure Related Durability of Cementitious Composites: Microdurability 2020* (pp. 446-453). Delft University of Technology.

Important note
To cite this publication, please use the final published version (if applicable).
Please check the document version above.

ASSESSMENT OF FREEZE-THAW RESISTANCE OF CEMENT BASED CONCRETE WITH GROUND GLASS – POZZOLAN THROUGH X-RAY MICRO TOMOGRAPHY

Marija Krstic (1), Julio F. Davalos (1), Emanuele Rossi (2), Stefan C. Figueiredo (2) and Oguzhan Copuroglu (2)

(1) Department of Civil Engineering, the City College of New York, the City University of New York, 160 Convent Avenue, New York, 10031 NY, USA

(2) Microlab, Faculty of Civil Engineering and Geosciences, Delft University of Technology, Stevinweg 1, 2628CN Delft, the Netherlands

Abstract

Over the last few years, the United States has experienced a shortage of fly ash and slag that consequently created a need for an alternative material that is locally available, sustainable, and provides desirable concrete properties. Recent studies have shown that Ground Glass Pozzolan (GGP) offers favorable attributes as a supplementary cementitious material (SCM) for concrete. However, there are limited studies demonstrating freeze-thaw (FT) resistance of concrete with GGP, as well as assessing the FT resistance in relation with the air-void system of GGP mixtures. In response, this study aimed to evaluate both macro- and micro-level behavior of GGP on FT resistance, and characterize mixtures with different contents of GGP. Six concrete mixtures were evaluated: three mixtures with 20, 30, and 40% GGP as cement replacements and three other reference mixtures with 30% fly ash and 40% slag and 100% Ordinary Portland cement (OPC). Following ASTM standards, concrete beam samples were tested for accelerated FT resistance and dynamic modulus of elasticity up to 1000 cycles. All concretes showed high FT resistance with a durability factor over 90% and, consequently, minimal deterioration and scaling. Core samples extracted from the FT conditioned beams were scanned with the X-ray micro-tomography (CT-scan) to identify air-void parameters. Through image analysis a quantification of air-void parameters was obtained, and their relationship to FT resistance was established. Using CT scan analysis, we demonstrated that concretes with the highest cement replacement with GGP and slag developed the most desirable spacing factor and specific surface for FT resistance.

Keywords: ground glass pozzolan (GGP), freeze-thaw resistance, durability factor, X-Ray micro tomography, air-void analysis

1. INTRODUCTION

Supplementary cementitious materials (SCMs), such as fly ash and granulated blast-furnace slag, are commonly used worldwide to produce more sustainable concrete with better mechanical and durability properties. The availability of fly ash in the USA has declined significantly due to recent environmental protection rules [1-2]. Slag is generally produced outside the USA and imported what makes it relatively expensive [3]. The shortage and cost of SCMs in the USA are of concern to the concrete industry. Consequently, there is a need for an alternate SCM to overcome the reduced supply of fly ash, particularly in the USA's Northeastern region. In recent years, the recycled soda-lime glass has received increased attention in the concrete industry since it can be effectively and economically transformed into pozzolanic material for concrete [4-7].

Freezing and thawing resistance is an essential durability property of concrete in inclement weather environments. Concrete structures are, besides mechanical loads, also exposed to environmental effects (e.g., low-temperature weather conditions), which can be damaging to porous brittle materials such as concrete. The durability of concrete is affected when subjected to repetitive freezing and thawing (FT) cycles, leading to accelerated deterioration and loss of stiffness and strength. Considering the freeze–thaw response, the most important factor of air void properties is pore interconnectivity. In normal concrete, the capillary pores (usually between 5 nm and 1 mm) are responsible for creating a network of voids [8]. Capillary forces in such small volumes are very important for allowing the water transport inside the paste matrix. One of the severe types of deterioration in concrete structures is associated with the cyclic volume expansion and contraction due to internal water freezing and thawing [9]. The volume expansion results in pressure build-up inside the pores if not accommodated with sufficient pore space and inter-connectivity in the matrix [10]. When the pressure exceeds the tensile strength of the cement paste at any point, it will lead to local cracking; hence the strength of concrete will decrease after several FT cycles [11].

Adding air-entraining agents is a well-known technique to improve the FT resistance. Compared to accidental entrapped air, entrained air bubbles are intentional and range from 1 µm to 100 µm [12]. Apart from increased air void content, it is believed that it is vital for freeze–thaw resistant concrete to have a spacing factor smaller than 0.2 mm (200 µm) and a specific surface of air void system greater than 24 1/mm [13]. Air void analysis is usually carried out as conventional testing method ASTM C457 [14], and it requires a tedious preparation of large samples dependent on aggregate size. Firstly, samples are viewed in 2D through an optical microscope or flatbed scanner [15], and then a standardized stereological method is applied (linear traverse method or point counting). X-ray computed tomography (CT-scan) can be also applied to characterize the air void system of cementitious materials, and it is a nondestructive method that uses high resolution for the characterization of materials in 3D [16]. It does not require elaborate sample preparation, however the limitation of micro CT is the size of samples that can fit into the machine and still accomplish an appropriate resolution to see the air voids [17].

There are limited studies [18] that have evaluated the freeze–thaw resistance of concrete with GGP replacements. Hence, this study aims to establish correlations among freeze–thaw resistance and air void parameters for concrete with different cement replacements with GGP. After the macroscopic characterization was completed, air void analysis was conducted using micro CT-scan to correlate macro and micro-evaluations. This work demonstrates a multiscale understanding of concrete durability properties with GGP as SCM, and the results contribute to practical implementations of concrete in inclement weather environments.

2. MATERIALS AND METHODOLOGY

This study evaluated six mixtures of air-entrained concrete for FT resistance up to 1000 cycles and air void system properties: three mixtures with 20, 30, and 40% GGP as cement replacements per weight, and three other reference mixtures with 30% fly ash (FA) and 40% slag (S) and 100% Ordinary Portland cement (OPC). The particle size distribution of cementitious raw materials, is presented in Table 1, and median particle size of OPC, S, FA and GGP is 14, 11, 15, and 10 µm respectively. Chemical composition (oxides and total alkalis) of raw cementitious materials was obtained with x-ray fluorescence (XRF) (see Table 2).

Table 1: Particle size distribution of raw materials

		OPC	**S**	**FA**	**GGP**
Mean:	µm	19.8	13.9	25.9	11.8
Median:	µm	14.2	11.3	14.9	10.0
S.D.:	µm	19.1	10.7	34.2	8.4
d10:	µm	2.9	2.1	3.3	2.3
d50:	µm	14.2	11.3	14.9	10.0
d90:	µm	45.7	30.0	65.4	24.2

Table 2: Chemical compositions of raw materials obtained through XRF.

Chemical Composition	**Ordinary Portland Cement (PC)**	**Slag (S)**	**Fly Ash Class F (FA)**	**Ground Glass Pozzolan (GGP)**
SiO_2, %	20.2	38.00	47.58	72.5
Na_2O, %	0.19	0.32	1.5	13.7
CaO, %	61.9	39.84	5.54	9.7
Al_2O_3, %	4.7	7.52	26.42	0.4
MgO, %	2.6	10.54	0.9	3.3
K_2O, %	0.82	0.38	1.9	0.1
Fe_2O_3, %	3.0	0.31	12.19	0.2
SO_3, %	3.9	0.16	1.08	0.1
Total alkalis $Na_2O + 0.658K_2O$, %	0.73	0.6	2.75	13.77

All six concretes were tested simultaneously for dynamic modulus and freeze-thaw resistance according to ASTM standards [19, 20]. X-ray micro computed tomography (Micro CT) was used to evaluate air-void properties of the same concrete mixtures (samples not exposed to freeze-thaw cycles). Micro CT- scanner was (Phoenix Nanotom, Boston, MA, USA), with digital GE DXR detector, and 3-D reconstruction was carried out with the software Phoenix datos|x 2.0. Core samples for air-void analysis (23 mm tall and 20 mm in diameter) were scanned with the voxel resolution of 10 µm, and the voltage and current of 140 kV and 170 µA respectively. The image analysis was performed with open source ImageJ [21], and there were two different approaches applied for calculating the air-void content for comparison of results. The first approach consisted of 2-D images equally spaced, 1 mm apart along the entire image stack (Figure 1 image 1.b). The assumption was made that air voids are not larger than 1 mm in vertical direction. For quantification of air void parameters; air content, spacing factor, specific surface, the linear-traverse method (ASTM C457 and EN 480-11) [14, 22], was downsized as shown in the Figure 1, (images 1.c through 1.f). The second approach was based on converting the entire stack of 1100 images into binary images and applying a threshold, black value for voids (0 GV) and white for everything else (256 GV). The area of voids was calculated as per each 2D image, and they were generated throughout the entire height of the image stack, 3D (see Figure 1, images 2.a through 2.d).

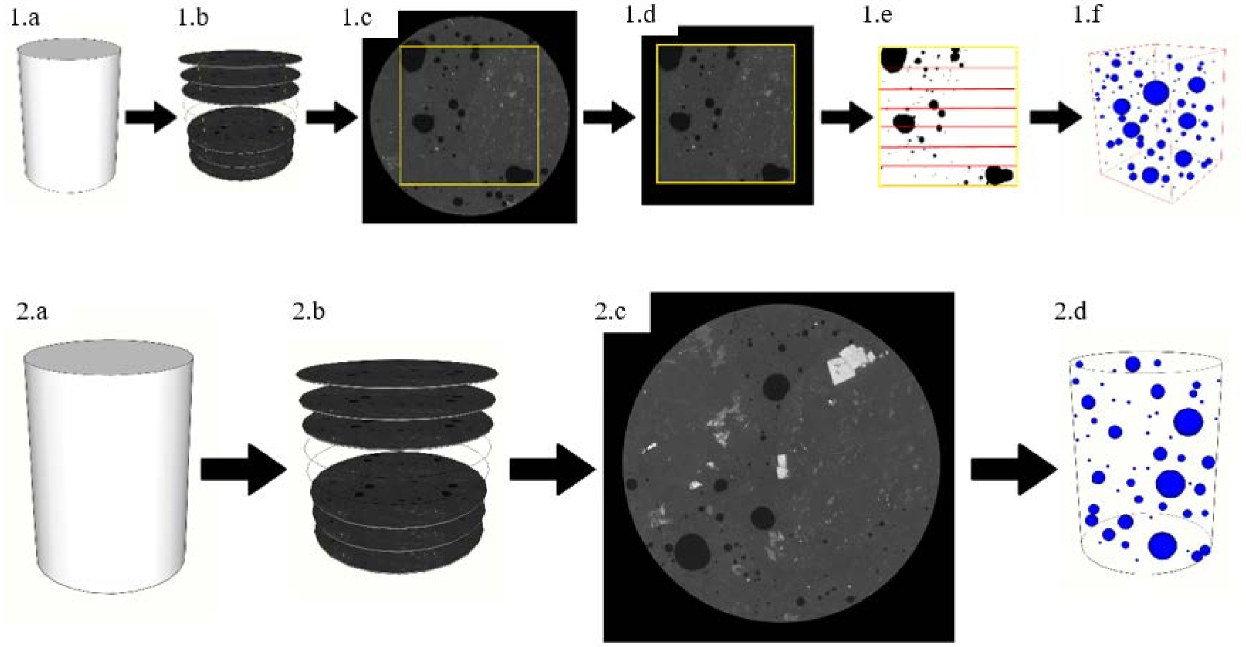

Figure 1: Approach 1.a-f: Downsized linear traversed method (2D), Approach 2.a-d: Threshold method of entire stack (3D). [23 24]

3. RESULTS AND DISCUSSION

3.1 Freeze-thaw resistance and dynamic modulus

The mass loss and durability factor are presented in Table 3. The mass loss was less than 1% for all concretes except for CM (1.6%). The durability factor was above 90% for all six concretes (0.9 for CM, and 0.94 for S-40 and G-40). The results indicate there was negligible deterioration of specimens, partly due to entrained air of ~6%. Although, it is widely recognized that air-entrainment enhances the freeze–thaw resistance of concrete, it was observed that the mixes with the highest cement replacement of 40% by S and GGP showed the highest durability factor and least mass loss of concrete (0.56, and 0.52 for S-40 and G-40 respectively).

Table 3: Durability properties.

	CM	G-20	G-30	S-40	G-40	FA-30
Mass Loss %	1.58	0.75	0.6	0.56	0.52	1.01
Durability factor	0.90	0.920	0.93	0.94	0.94	0.91

3.2 Air-void analysis of hardened concrete using x-ray computed tomography

Air content of fresh concrete and air-void content of hardened concrete by both approaches were compared for all six concrete mixtures and summarized in Figure 2. The difference in results could be due to numerous reasons, a slightly different geometry of a sample considered for calculating air content, or in the case of a linear traverse method it is possible that human error can likely occur. The Threshold method of an entire stack did not account for any voids smaller than 50 µm, while the linear traverse method did. The linear traverse method applied through micro CT-scan is a tedious procedure and it is difficult to make a decision as to whether the air voids are smaller than 50 µm, so it is easier to account for all of them. Therefore, it is reasonable that the linear traverse method gives a slight overestimation of the air void content [24].

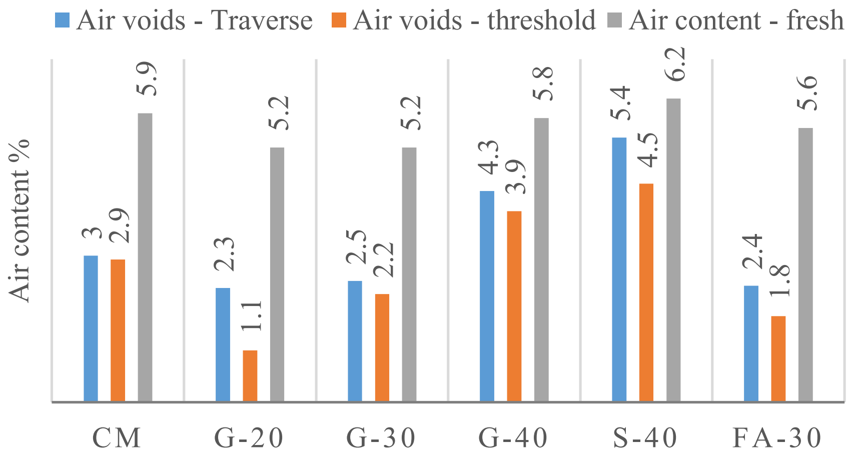

Figure 2: Summary of air void content obtained with different methods.

The spacing factor L (mm) is presented in Figure 3, and shows that all concretes had smaller than 0.3 mm except for CM (0.45 mm). Both S-40 and G-40 had the spacing factor smaller than recommended 0.2 mm (0.15 mm and 0.19 mm, respectively). Results for specific surface α, are presented in Figure 4. CM had only 11.9 1/mm, while S-40 had 26.2 1/mm. Both G-20 and FA-30 had ~21 1/mm, while G-30 and G-40 measured ~24 1/mm. The linear traverse method, showed negligibly higher percent air void content than the approach completely based on Threshold of an entire stack (see Figure 2). From the air void analysis it was also demonstrated that G-40 and S-40 showed the most desirable parameters prescribed for freeze–thaw resistant concrete as measured by spacing factor smaller than 0.2 mm and specific surface greater than 24 1/mm [13]. According to this study 40% GGP replacement showed that it is as successful as 40% S to improve the FT resistance of concrete, by maintaining a recommended spacing factor and specific surface which are crucial parameters.

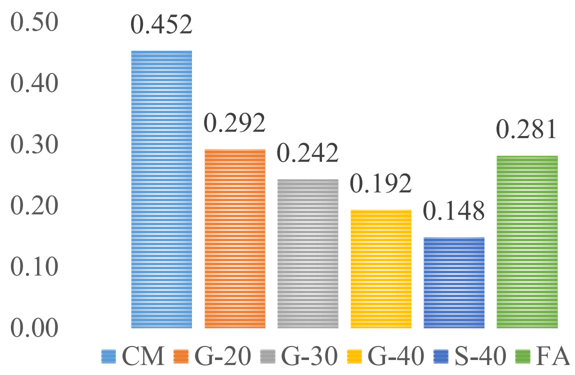

Figure 3: Spacing factor of all concretes L (mm)

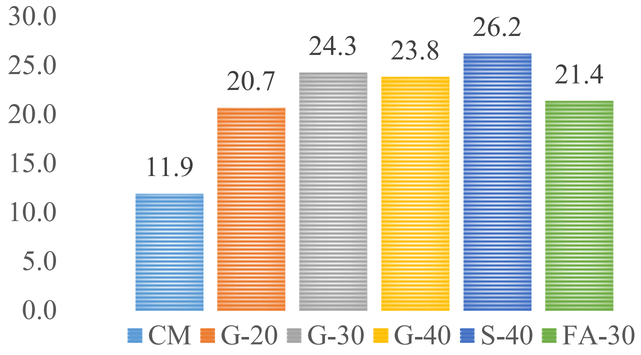

Figure 4: Specific surface of all concretes α (1/mm)

4. CONCLUSION

This study is a succinct summary [24] of an assessment of the freeze–thaw resistance of concretes containing cement replacement by GGP of up to 40% by weight, and comparing the performance with fly ash and slag. Macroscopic properties such as air content of fresh concrete, mass loss, and durability factor were attained through standard ASTM methods. The air void properties of hardened concretes that were not exposed to freeze-thaw cycles, were evaluated with X-ray computed tomography, and the image analysis was performed with ImageJ. Based on the combined macro and micro-evaluations of concretes with GGP in this study, the following conclusions can be drawn:

- A mass loss of ~1%, and durability factor of above 90%, for all concretes except for CM, indicated improved freeze–thaw resistance with increased cement replacements by GGP regardless to air-entraining agent, due to its pozzolanic activity, and perhaps consuming more CH for C-S-H formation.

- Using GGP as an alternate SCM, serves as nucleation for air bubbles due to its angular particle shape and finer particle size than CM, and subsequently its larger specific surface area. With higher cement replacement with GGP, spacing factor decreases and specific surface increases, which are favorable for FT resistance.
- The air void analysis by micro CT-scan coupled with ImageJ can be successfully utilized for evaluating the microstructure of cementitious materials. It is a nondestructive method, and it can provide 3D information that is especially useful for air void analysis. This method requires minimum sample preparation, unlike the standard method ASTM C457; however, it has a limitation on a sample size.

ACKNOWLEDGEMENTS

We gratefully acknowledge the collaboration and supply of commercial GGP *Pozzotive* by Urban Mining Northeast. We thank the contributions and input from Building Product Ecosystems, LLC. We appreciate the generous help and guidance from the technical team at the Microab at Delft University of Technology in the Netherlands. We also thank the DURST Organization for partial funding of the project.

REFERENCES

[1] Roston E.; and Migliozzi, B. "Obama's EPA Rule Is Redrawing the U.S. Coal Map," *Bloomberg New Energy Finance-US coal retirements database*, 2015: http://www.bloomberg.com/graphics/2015-coal-plants/.
[2] Sheikh, V. Limited Availability of Cementitious Materials Could Impact the Value Chain. *Appl. Sci. Sustain. Coal Ash* **2018**, 34–36.
[3] Ober, J.E. U.S. Geological Survey, "Mineral Commodity Summaries," 2017: https://www.usgs.gov/centers/nmic/arsenic-statistics-and-information#mcs.
[4] Kamali, M.; Ghahremaninezhad, A. An investigation into the hydration and microstructure of cement pastes modified with glass powders. *Constr. Build. Mater.* **2016**, *112*, 915–924.
[5] Krstic, M.; Davalos, J.F. Field application of recycled glass pozzolan for concrete. *ACI Mater. J.* **2019**, *116*, 123–131.
[6] Krstic, M.; Davalos, J.F. Macro-and Micro-structure Evaluations of Recycled Post-consumer Glass Cementitious Material for Concrete. In *Proceedings of the Interdisciplinary Approaches for Cement-based Materials and Structural Concrete: Synergizing Expertise and Bridging Scales of Space and Time*; Miguel, A., Dirk Schlicke, F.B., Jędrzejewska, A., Eds.; RILEM Publications: Madeira Island, Portugal, 2018; pp. 261–266.
[7] Kaminsky, A.; Krstic, M.; Rangaraju, P.; Hamou, A.T.; Thomas, M. Ground-Glass Pozzolan for Use in Concrete, Members of ASTM Subcommittee C09.24 summarize industry context behind new ASTM standard specification. *Concr. Int.* **2020** *42*, 24-32.
[8] Pawlowicz, J. Evaluation of Air Entraining Behaviour in Concrete Using Computer Aided Methods on Hardened Samples. Master's Thesis,TU Delft University, Delft, The Netherlands, 2019.
[9] Hanjari, K.Z.; Utgenannt, P.; Lundgren, K. Experimental study of the material and bond properties of frost-damaged concrete. *Cem. Concr. Res.* **2011**, *41*, 244–254.
[10] Neville, A.M. *Properties of Concrete*; Pearson Education Limited: London, UK, 2011; ISBN 978-0-273-75580-7.

[11] Shang HS, S.Y. Experimental study of strength and deformation of plain concrete under biaxial compression after freezing and thawing cycles. *Cem. Concr. Res.* **2006**, *36*, 1857–1864.

[12] Gagne; R *Science and Technology of Concrete Admixtures*; Elsevier: Amsterdam, The Netherlands, 2016; ISBN 9780081006931.

[13] Saucier, F., Pigeon, M., Cameron, M. Air-void stability-part V: Temperature, general analysis, and performance index. *ACI Mater. J.* **1991**, *88*, 25–36.

[14] ASTM C 457-12 Standard Test Method for Microscopical Determination of Parameters of the Air-Void System in Hardened Concrete 1. *ASTM Int.* **2013**, *05*, 15 pages.

[15] Peterson, K.W.; Anzalone, G.C.; Nezami, S.; Oh, C.Y.S.; Lu, H. Robust Test of the Flatbed Scanner for Air-Void Characterization in Hardened Concrete. *J. Test. Eval.* **2016**, *44*, 20140432.

[16] Kim, K.Y.; Yun, T.S.; Choo, J.; Kang, D.H.; Shin, H.S. Determination of air-void parameters of hardened cement-based materials using X-ray computed tomography. *Constr. Build. Mater.* **2012**, *37*, 93–101.

[17] Lanzón, M.; Cnudde, V.; De Kock, T.; Dewanckele, J. X-ray microtomography (μ-CT) to evaluate microstructure of mortars containing low density additions. *Cem. Concr. Compos.* **2012**, *34*, 993–1000.

[18] Omran, A.; Tagnit-hamou, A. Performance of glass-powder concrete in field applications. *Constr. Build. Mater.* **2016**, *109*, 84–95.

[19] *ASTM C215*; *Standard Test Method for Fundamental Transverse, Longitudinal, and Torsional Resonant Frequencies of Concrete Specimens,* ASTM: West Conshohocken, PA, USA, 2015; volume 4.02, 7 pages.

[20] *ASTM C666*; *Standard Test Method for Resistance of Concrete to Rapid Freezing and Thawing* ASTM: West Conshohocken, PA, USA, 2015.

[21] Rueden, C.T.; Schindelin, J.; Hiner, M.C.; DeZonia, B.E.; Walter, A.E.; Arena, E.T.; Eliceiri, K.W. ImageJ2: ImageJ for the next generation of scientific image data. *BMC Bioinformatics* **2017**, *18*, 1–26.

[22] NEN-EN 480-11, Admixtures for concrete, mortar and grout- Test methods Part 11: Determination of air void characteristics in hardened concrete. TU Delft, The Netherlands,**2005**; Volume 11, European Committee for Standardization, Brussels, Belgium, 25 pages.

[23] Krstic, M. Macro- and Micro-structure Evaluations and Field Applications of Concrete with Recycled Glass. Ph.D. Thesis, The CIty College of New York: CUNY, New York, NY, USA, 2020.

[24] Krstic, J. F. Davalos, E. Rossi, Stefan C. Figueiredo, O. Copuroglu, “Freeze-Thaw Resistance and Air-Void Analysis of Concrete with Recycled Glass – Pozzolan Using X-Ray Micro Tomography,” MDPI Materials Journal, (2021)